焊接残余应力对 P92钢 Ⅳ型蠕变开裂的影响

姜运建[1,2,3], 荆洪阳[1,2], 徐连勇[1,2], 王 庆[3], 代 真[3]

(1. 天津大学 材料科学与工程学院, 天津 300072;
2. 天津市现代连接技术重点实验室, 天津 300072; 3. 河北省电力研究院, 石家庄 050021)

摘 要: P92钢焊接接头在高温长时服役条件下易于在细晶热影响区(FGHAZ)或临界热影响区(ICHAZ)产生 Ⅳ型裂纹. 但对于 Ⅳ型开裂的机理, 至今尚未达成一致认识. 为了科学地认识 Ⅳ型开裂, 文中采用大型有限元软件 ABAQUS对 P92钢焊接接头的温度场、应力场以及蠕变进行了有限元模拟, 并且通过 X射线测量试验对残余应力模拟值进行了验证. 结果表明, 通过温度场模拟, 得到了 FGHAZ与 ICHAZ的准确位置; 焊接残余应力最大值集中在 FGHAZ和 ICHAZ, 并且轴向蠕变应变分布规律与焊接残余应力相一致. 因此焊接残余应力的集中, 是导致焊接接头蠕变应变聚集和 Ⅳ型开裂的关键因素之一.

关键词: P92钢; Ⅳ型裂纹; 温度场; 焊接残余应力; 有限元模拟

中图分类号: TG404 文献标识码: A 文章编号: 0253-360X(2011)01-0016-05

姜运建

0 序 言

随着国家电力工业发展战略的确定, 超(超)临界机组将成为中国火电机组建设的主导方向. 目前, 铁素体耐热钢(T/P92, T/P91)正逐步进入国家火力发电行业.

主蒸气管道等所使用的 P92, P91钢, 长期服役于高温、高压环境下, 其焊接接头最重要的失效方式—发生于细晶热影响区(FGHAZ)或临界热影响区(ICHAZ)内的恶性早期 Ⅳ型蠕变开裂, 已严重威胁高温构件的安全可靠运行. 国内外已开展了大量相关研究, 但对这种 Ⅳ型开裂的条件和机制, 目前尚未形成一致的认识.

已有研究表明, 焊接接头的不均匀性引起的蠕变量的错配以及其应力水平对于 Ⅳ型裂纹的产生有着重要影响[1]. 焊接时 FGHAZ和 ICHAZ受较低的温度循环, 在拘束条件下, 蠕变孔洞和裂纹的形核长大速度较快, 从而降低强度[2]. FGHAZ和 ICHAZ内碳化物粗化, 不仅降低了固溶强化的效果, 同时还降低了沉淀强化的作用, 从而导致了焊接接头中该区域蠕变强度的下降[3]. 但关于焊接接头应力水平的影响尚处于研究之中. 而采用数值模拟技术对焊接残余应力的分布特点进行预测不失为一种探求之法.

文中利用 ABAQUS有限元软件, 对 P92钢的焊接过程进行了数值模拟, 得到了焊接温度场的分布规律, 并研究了焊接残余应力对 Ⅳ型蠕变的影响.

1 物理模型

研究对象是直径为 φ355 mm, 壁厚为 40 mm的 P92钢主蒸气管道, 管内介质温度为 600 ℃, 压力为 26 MPa. 焊缝坡口为 VY型, 焊接结束后冷却至室温, 焊接接头如图 1所示.

图 1中第 1层、第 2层为氩弧焊焊接, 预热温度为 100~200 ℃, 层间温度为 150~250 ℃. 第 3层以上为焊条电弧焊焊接, 层间温度约为 200 ℃. 所使用的焊丝及焊条均为 MTS616. 具体焊接工艺参数如表 1所示.

表 1 焊接工艺参数

Table 1 Welding parameter

焊道	焊条直径 d/mm	焊接电流 I/A	电弧电压 U/V	焊接速度 v/(mm·s⁻¹)
1~2层	2.4	100~120	11~15	1.00
3~4层	2.5	80~110	22~24	2.17
5层以上	3.2	110~130	24~26	2.34

收稿日期: 2009-09-16

基金项目: 国家自然科学基金资助项目(50805103); 天津市自然科学基金资助项目(08JCZDJC18100)

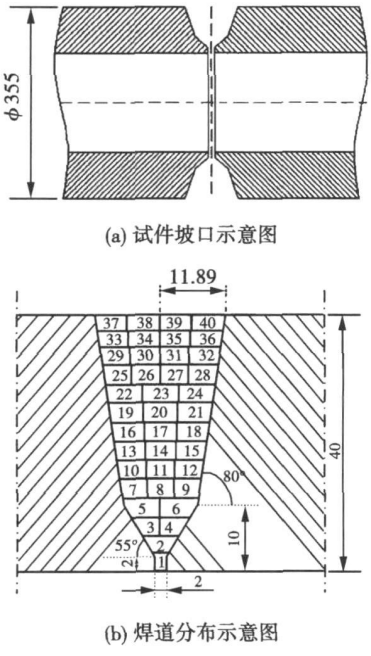

图 1　管道焊接接头（mm）

Fig. 1　Pipe welded joint

2　有限元模拟

2.1　分析模型及网格划分

管道对接焊结构简单，且焊接接头的轴向应力水平一直是大家关注的领域．基于这点，对焊接接头的数值模拟可采用二维模型，这样既节约了建模时间，又完全满足对关注点仔细考察的目的．利用 ABAQUS网格自适应处理的特点，在焊缝和热影响区网格划分比较密集，而在远离焊缝处网格比较稀疏，如图 2所示．文中为多层多道焊，轴对称模型已不能满足需求，因此采用二维平面模型，其中节点 9 963个，单元 9 680个．计算焊接温度场采用 DC2D4单元，计算残余应力场与蠕变采用平面应变（CPE4）单元．计算程序中，运用单元生死技术（element birth technique）来实现多道焊模拟．

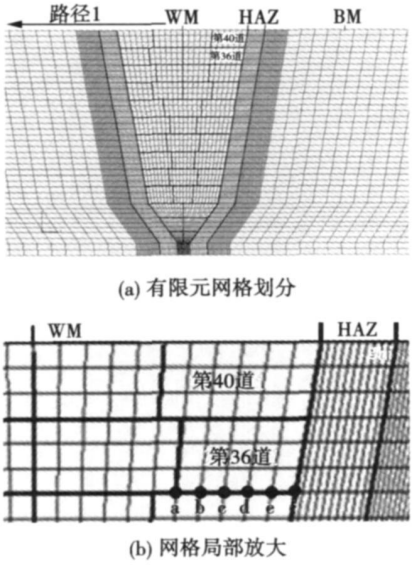

图 2　有限元模型网格划分及其局部放大

Fig. 2　Mesh of finite element model and local enlarging

2.2　材料性能参数

管道的材料为 P92钢，计算时可认为焊材和母材的材料相同．并且假定其物理性能在 700～1 900 ℃时保持不变[4]，具体的材料性能如图 3所示[5]，其中 c_p为比热容（10^2 J/(kg·K)）；λ为导热系数（10 W/(m·K)）；α_l为线膨胀系数（10^{-5}/K）；E为弹性模量（10^2 GPa）；μ为泊松比；σ为屈服强度（10^2 MPa）．蠕变计算时采用 ABAQUS软件自带的材料本构模型，即

$$\dot{\varepsilon} = B\sigma^n \tag{1}$$

式中：$\dot{\varepsilon}$为蠕变应变率；σ为单轴应力；B，n均为材料常数．该材料的蠕变性能参数可以通过单轴蠕变试验获得[2]．

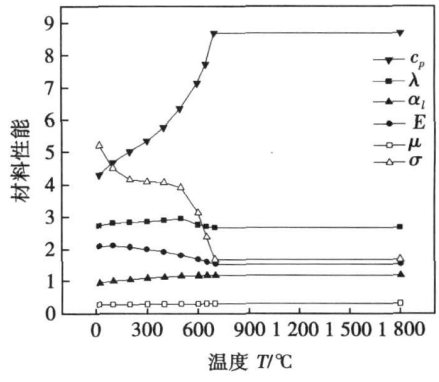

图 3　P92钢材料性能参数

Fig. 3　Performance parameters of P92 steel

2.3　边界条件及初始条件

在温度场计算中，焊件的初始温度取室温 20 ℃，焊接过程中，焊件与外界同时存在着对流和辐射换热，因此焊件的内、外表面均施加对流和辐射边界条件，对流系数取 10 W/(m²·K)，辐射发射率为 0.85[6]．在焊接残余应力场分析中，为了确保焊件不发生刚性移动，在管道模型的两个端面约束所有的自由度．

3　数值模拟结果与分析

3.1　焊接温度场

厚壁 P92钢在多层多道焊接过程中，750 ℃的回火温度可以保证焊缝具有较高的冲击韧度，因此，

应该保证后一层焊道对前一层焊道起到回火作用. 图 2标出了焊缝区 (WM)、热影响区 (HAZ)、母材区 (BM)以及焊道的分布. 从图 2图 4可以看出第 40焊道施焊时,第 36道的最底部节点 a~处热循环曲线峰值温度均超过 750 ℃,即 P92钢的回火温度,亦即可以满足后一层焊道对前一层焊道起到回火作用. 从而验证了此焊接工艺的可行性.

对于焊接接头的 Ⅳ型裂纹而言,产生于细晶热影响区 (焊接峰值温度 $T_m > A_{c_3}$)和临界热影响区 (焊接峰值温度 $T_m = A_{c_1} \sim A_{c_3}$). 根据 P92钢的冶金学特点,其 A_{c_1}的温度在 800~835 ℃之间; A_{c_3}的温度在 900~920 ℃之间[7,8]. 第 40焊道施焊时, g节点处热循环曲线峰值温度达到 900 ℃, h节点处热循环曲线峰值温度达到 850 ℃, i节点处热循环曲线峰值温度达到 800 ℃,见图 4. 可以确定 g点处于细晶热影响区与临界热影响区之间,亦即 Ⅳ型蠕变开裂的产生区域.

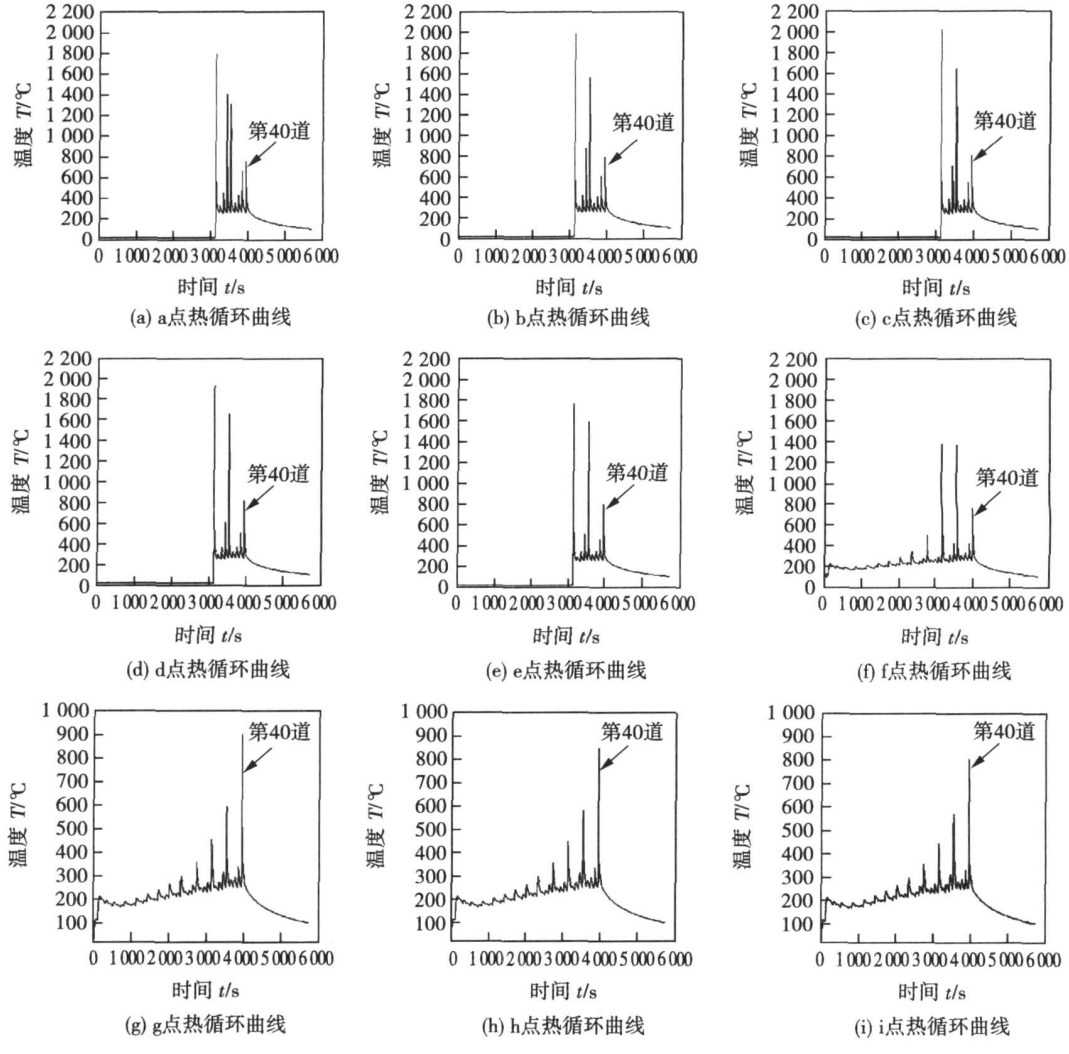

图 4 热循环曲线

Fig. 4 Thermal cycling curve

3.2 应力场

图 5为轴向残余应力 ($\sigma_{S_{11}}$)和 Mises应力分别着沿管道外壁 (路径 1)的分布图,模拟范围为起于焊缝中心线,止于距焊缝中心线 45 mm处.

其中可以看出轴向应力 $\sigma_{S_{11}}$在模拟范围内始终表现为拉应力. 在焊缝区,应力值最小为 35.14 MPa,自中心线向焊缝边缘呈逐渐增大趋势; 在热影响区, g点附近 (至焊缝中心线距离 13.94 mm位置)出现应力最大值,高达 242.92 MPa; 在母材区,远离焊缝处,应力逐渐衰减至 4.85 MPa. Mises应力在模拟范围内呈拉应力状态,并且其变化趋势与轴向应力相同,最大值约为 431.43 MPa,仍出现在 g点附近 (至焊缝中心线距离 13.93 mm位置).

文中模拟了管道运行 1.0×10^5 h时,轴向蠕变应变 ($\varepsilon_{CR_{11}}$)沿路径 1的分布情况,如图 6所示. $\varepsilon_{CR_{11}}$

与图 5中的轴向应力 $\sigma_{S_{11}}$分布规律几乎完全一致：高应力区域，其轴向蠕变变形量亦较大，即在 g点附近（至焊缝中心线距离 13.94 mm处），蠕变应变量达到最大值，为 1.7%；而在远离焊缝的母材区，$\varepsilon_{CE_{11}}$逐渐衰减至 0.3%．这表明管道蠕变变形与焊接残余应力密切相关，焊接残余应力是影响焊接接头蠕变变形的主要因素之一．

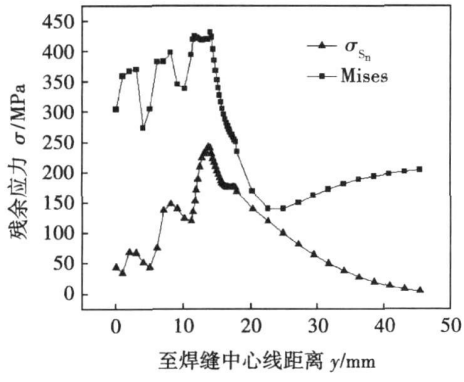

图 5　沿路径 1的焊接残余应力

Fig. 5　Welding residual stress along path 1

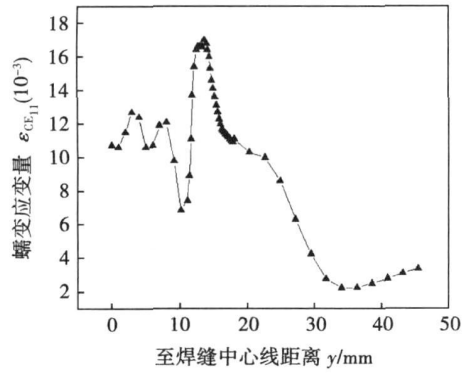

图 6　沿路径 1的蠕变应变

Fig. 6　Creep strain along path 1

综上所述，焊接过程中（第 40焊道施焊时），g节点热循环曲线峰值温度达到 900 ℃，亦即该点位于细晶热影响区与临界热影响区之间．同时，g节点处存在较高的初始焊接残余应力，并呈拉应力状态；而且受焊接残余应力影响，轴向蠕变应变最大值也出现在 g点处．因此焊接接头细晶热影响区与临界热影响区的焊接残余应力集中将与焊接接头的 Ⅳ型蠕变开裂有密切关系．

4　结果验证

采用 X射线衍射技术测量了规格为 φ550 mm×80 mm的 P92管道外表面的轴向焊接残余应力（图 7），该管道与文中模型相比，均属厚壁管道焊接，且规格、坡口形式、焊接参数近乎相同，因此具有一定的参考价值．试验点布置规律如下：试验范围为自焊缝中心线起，截止于距焊缝中心线 78 mm处．焊缝区自焊缝中心线起共布置 6个测点，相互间隔为 3 mm；热影响区共 3个测点，相互间隔为 1.5 mm；母材区分为两部分，一部分为靠近热影响区的区域，布置 3个测点，相互间隔为 3 mm；另一部分为远离热影响区的区域，布置 8个测点，相互间隔为 6 mm．可以看出试验点的轴向残余应力变化规律与模拟结果一致，试验范围内均为拉应力，轴向残余应力最大值同样出现在靠近母材的热影响区内，约为 187.5 MPa，而在焊缝区和母材区残余应力都有所降低．

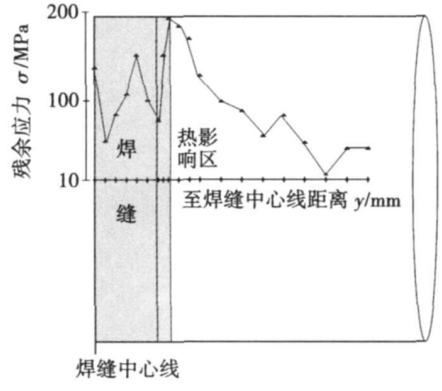

图 7　轴向残余应力的试验点

Fig. 7　Experimental result of axial residual stress

5　结　　论

（1）利用 ABAQUS软件，对 P92钢焊接接头进行了有限元模拟，得到了温度场、焊后残余应力与蠕变应变的分布规律．

（2）通过对焊接热循环曲线峰值温度的分析，在焊接过程中可以满足后一层焊道对前一层焊道起到回火作用，并得到了细晶热影响区和临界热影响区确切位置，该区域是 Ⅳ型裂纹容易出现的部位．

（3）轴向焊接残余应力和 Mises应力在焊缝和热影响区内均呈拉应力状态，并且其最大值均集中在焊接接头的细晶热影响区和临界热影响区；采用 X射线衍射技术测量了该管道外表面的轴向残余应力，试验结果与模拟值相同．同时运行 10^5 h的轴向蠕变应变分布趋势与残余应力近乎一致．因此焊接残余应力决定了轴向蠕变，并最终导致了 Ⅳ型

裂纹.

(4)对于新型耐热钢,焊后应采用适当方法降低焊接残余应力,以减少应力集中对材料焊接接头处的损伤.

参考文献:

[1] Allen D J, Harvey B, Brett S J. Four crack-an investigation of the creep performance of advanced high alloy steel welds[J]. International Journal of Pressure Vessels and Piping, 2007, 84(1-2): 104-113.

[2] Takashi Watanabe, Masaaki Tabuchi, Masayoshi Yamazaki, et al. Creep damage evaluation of 9Cr-1Mo-V-Nb steel welded joints showing type IV fracture[J]. International Journal of Pressure Vessels and Piping, 2006, 83(1): 63-71.

[3] Francis J A, Mazur W, Bhadeshia H K D H. Type IV cracking in ferritic power plant steels[J]. Materials Science and Technology, 2006, 22(12): 1386-1395.

[4] 张国栋, 薛吉林, 周昌玉. 基于正交试验设计的高温管道焊接工艺优化[J]. 焊接学报, 2008, 29(11): 53-56.
Zhang Guodong, Xue Jilin, Zhou Changyu. Optimization on welding procedure of high temperature pipeline based on orthogonal test design[J]. Transactions of the China Welding Institution, 2008, 29(11): 53-56.

[5] 王崇斌, 徐 沁. 亚临界和超临界锅炉高温过热器用 NF616 钢性能[J]. 锅炉技术, 1995, 26(12): 13-20.
Wang Chongbin, Xu Qin. Properties of NF616 steel in HT superheater of sub-critical and super-critical boilers[J]. Boiler Technology, 1995, 26(12): 13-20.

[6] 蒋文春, 巩建鸣, 唐建群, 等. 焊接残余应力下氢扩散的数值模拟[J]. 焊接学报, 2006, 27(11): 57-60, 64.
Jiang Wenchun, Gong Jianming, Tang Jianqun, et al. Numerical simulation of hydrogen diffusion under welding residual stress[J]. Transactions of the China Welding Institution, 2006, 27(11): 57-60, 64.

[7] 乔亚霞, 武英利, 徐联勇. 9%-12% Cr高等级耐热钢的Ⅳ型开裂研究进展[J]. 中国电力, 2008, 41(5): 33-36.
Qiao Yaxia, Wu Yingli, Xu Lianyong. Research progress on type Ⅳ cracking of 9% ~ 12% Cr high-grade heat-resisting steel[J]. Electric Power, 2008, 41(5): 33-36.

[8] 王红鸿, 张汉谦, 孙 咸. 9% Cr-1% Mo耐热钢焊缝金属显微组织特征解析[J]. 焊接学报, 2008, 29(9): 91-95.
Wang Honghong, Sun Hanqian, Sun Xian. Analysis of microstructure characteristic of 9% Cr-1% Mo heat resistant steel weld metal[J]. Transactions of the China Welding Institution, 2008, 29(9): 91-95.

作者简介:姜运建,男,1963年出生,博士研究生,国际焊接工程师.主要从事电站高温设备寿命评价技术研究.发表论文 8篇.Email: jiangyunjian@yahoo.cn

[上接第 15页]

[3] 郑韶先, 朱 亮, 张旭磊, 等. 焊剂带约束电弧在超窄间隙中的加热特性[J]. 焊接学报, 2008, 29(5): 57-60.
Zheng Shaoxian, Zhu Liang, Zhang Xulei, et al. Heating characteristic of constricting arc with flux strips in ultra-narrow gap welding[J]. Transactions of the China Welding Institution, 2008, 29(5): 57-60.

[4] 郑韶先, 朱 亮, 黄斌维, 等. 焊剂带约束电弧用于超窄间隙的焊接[J]. 机械工程学报, 2009, 45(2): 219-223.
Zheng Shaoxian, Zhu Liang, Huang Binwei, et al. Constricted arc by flux strips applied to ultra-narrow gap welding[J]. Chinese Journal of Mechanical Engineering, 2009, 45(2): 219-223.

作者简介:郑韶先,男,1978年出生,副教授,博士.主要从事焊接工艺及电弧物理的研究.发表论文 9篇.Email: zhengsx2008@mail.lzjtu.cn

MAIN TOPICS, ABSTRACTS & KEYWORDS

Research and development of a new submerged arc welding wire for X100 pipeline steel ZHANG Min, LÜ Jinbo, WANG Chao, LI Jihong (School of Material Science and Engineering, Xi'an University of Technology, Xi'an 710048, China). p. 1—4, 8

Abstract: According to the nucleate mechanics of acicular ferrite and bainite in high strength low alloy steels (HSLA) welded deposit, Mn-Ni-Mo-Cr was chosen as main alloy elements and Ce, Ti, B as micro-alloy elements which accelerate the nucleate of acicular ferrite. The content of C, Si, P, S, N elements was reduced and C to be the level of ultra-low carbon to meet the large energy input welding and to ensure the content of Mn, Mo, Cr to compensate for intensity loss brought by reduced C, Si. By in addition, Ti and B were added to avoid producing excessive acicular ferrite which would reduce the intensity or cause segregation of alloy elements to decrease the toughness of weld joint and proper Cu to enhance the ability of weld joint to resist the atmospheric corrosion. As the results, the developped welding wire matching flux SJ101-G, had the microstructure of deposited metal was acicular ferrite and lath bainite mainly in which a small amount of granular bainite precipitated and dispersed.

Key words: SAW; acicular ferrite; granular bainite; strength and toughness

Microstructure and high-temperature wear-resistance of nitrogen-alloying hardfacing alloy YANG Ke[1,2], YU Shengfu, YANG Hua[1] (1. College of Mechanical and Electrical Engineering, Hehai University, Changzhou, Jiangsu 213022, China; 2. Province Key Lab of Advanced Welding Technology, Jiangsu University of Science and Technology, Zhenjiang, Jiangsu 212003, China; 3. College of Materials Science and Engineering, Huazhong University of Science and Technology, Wuhan 430074, China; 4. Shanghai Jiaowang Shipbuilding Technology Development Co., Ltd., Shanghai 200136, China). p. 5—8

Abstract: The hardfacing alloy of martensitic stainless steel added nitrogen as alloying element was made, and the microstructure and high-temperature wear-resistance was also studied. It is found that the hardfacing alloy has two main phases of martensite and carbonitrides. The high-temperature wear mechanism between hardfacing alloy of the martensitic stainless steels and the low-carbon steel was abrasive wear because the effect of oxide formation on the surface of the low-carbon steel. The oxide was sticking on the surface of hardfacing alloys and increasing the abrasive wear damage. The results showed that carbonitride particles distributed homogeneously in the hardfacing alloy and had a good strengthening effect on the hardness and high-temperature wear resistance.

Key words: martensitic stainless steel; hardfacing alloy; carbonitride; high-temperature wear

Effects of rare earth Ce on microstructures of Ag30CuZnSn-3Ga-2In filler metal LAI Zhongmin, WANG Jianxin, LIU Fangyan[2] (1. Province Key Lab of Advanced Welding Technology, Jiangsu University of Science and Technology, Jiangsu Zhenjiang 212003, China; 2. Lucas Milhaupt (Suzhou) Co., Ltd., Jiangsu Suzhou 215122, China). p. 9—12

Abstract: The cadmium-free silver filler metal Ag30CuZnSn-3Ga-2In has excellent comprehensive property. In this paper, the effects of rare earth, called usually "vitamin" of metals, Ce on microstructures of Ag30CuZnSn-3Ga-2In filler metal were studied. Results showed that the rare earth Ce did not dissolve into Ag based solid solution and Cu based solid solution, but could form rare earth Phase which acted as the particle of "out of Phase nucleation" in the filler metal matrix. Enrichment phenomena could be confirmed for rare earth Ce in the grain boundary. It is found that rare earth Ce can fine grain strengthen grain boundary and exhibit the formation of Cu_6Sn_5 for the silver filler metals bearing Ga and In. It is found that adding 0.1% rare earth Ce can improve the microstructure of the Ag30CuZnSn-3.0Ga-2.0 filler metals greatly.

Key words: rare earth Ce; silver filler metal; microstructure; out of Phase nucleation

Relationship between position of flux strips in arc zone of ultra-narrow gap and constricting arc ZHENG Shaoxian, ZHU Liang, CHEN Jianhong (1. School of Mech-Electronic Technology, Lanzhou Jiaotong University, Lanzhou 730070, China; 2. State Key Laboratory of Gansu Advanced Non-ferrous Metal Materials, Lanzhou University of Technology, Lanzhou 730050, China). p. 13—15, 20

Abstract: When flux strips applied to constrict arc have different relative positions with arc in ultra-narrow gap, flux strips can cause different constricting effects on arc, so the position of flux strips in the arc zone is the linchpin of constricting arc in time of ultra-narrow gap welding with flux strips constricting arc. By analyzing the position of flux strips in the arc zone, the results indicate only when three positional conditions are satisfied, flux strips can efficiently constrict arc: firstly, flux strips need cling to sidewalls in the direction of radial of arc; secondly, flux strips need proper action length in the direction of arc length; thirdly, the tip of wire needs be located in the center of flux strips. Furthermore, under arc current exceeds 240 A, flux strips can easily cling to the surface of wire because of action of electromagnetic force; the position of flux strips in the direction of radial of arc can be located efficiently by supporting flux strips.

Key words: flux strips constricting arc; ultra-narrow gap welding; position of flux strips

Effect of welding residual stress on type IV creep failure of P92 steel JIANG Yunjian[1,2,3], JING Hongyang[2], XU Li-

anyong[2], WANG Qing, DAI Zhen[3] (1. School of Material Science and Engineering, Tianjin University, Tianjin 300072, China; 2. Tianjin Key Laboratory of Advanced Joining Technology, Tianjin 300072, China; 3. Hebei Electric Power Research Institute, Shijiazhuang 050021, China). p. 16—20

Abstract: Type IV cracking is considered to be the likely failure mode of P92 steel welds when operated at high temperature for long duration. Type IV failure often takes place at the intercritical heat affected zone (ICHAZ) or fine grained heat affected zone (FGHAZ). However, the mechanism of type IV cracking has not yet been understood unequivocally. In order to investigate type IV failure scientifically, temperature field, welding residual stress and creep strain for welded joint of P92 steel are simulated by ABAQUS code. Experimental result obtained from X-ray diffraction technique is conducted to verify the simulation. The research results show that the locations of ICHAZ and FGHAZ are demonstrated according to the simulation of temperature field. Maximal residual stress concentrates in the ICHAZ and FGHAZ. And axial creep strain is in good agreement with residual stress. So concentration of residual stress that results in accumulation of creep strain and type IV cracking is regarded as remarkable factor.

Key words: P92 steel; type IV cracking; temperature field; welding residual stress; finite element simulation

Relations between 3-dimension interface topography with thermal stress of thermal barrier coatings

WANG Zhiping, HAN Zhiyong, CHEN Yajun, DING Kunying (Institute of Material Technology, Civil Aviation University of China, Tianjin 300300, China). p. 21—24

Abstract: Double layer thermal barrier coatings (bond coating is NiCrAlY and ceramic coating is ZrO_2) was prepared by atmospheric plasma sprayed method. Using ABAQUS software, the thermal stress distribution of 3-dimension ellipse interface topography between bond coating and ceramic coating was numerically simulated by indirect coupling method. Relations between thermal stress with location and size of ellipse topography unit were obtained. The calculating results show that the stress is affected by location and size obviously and stress of boundary topography unit is bigger than that of center unit when the size of unit is invariable. The boundary topography units are danger unit and corner points are danger points. The stress of danger point reaches 324 MPa when short half-axes is 20.

Key words: thermal barrier coatings; thermal stress; interface topography

Master-slave coordinated motion controlling of double-sided arc welding robots

ZHANG Huajun[3], ZHANG Guangjun[2], CAI Chunbo[1], XIAO Jun[2], GAO Hongming (1. School of Materials Science and Engineering, Harbin University of Science and Technology, Harbin 150040, China; 2. State Key Laboratory of Advanced Welding Production Technology, Harbin Institute of Technology, Harbin 150001, China; 3. School of Material Science and Technology, Shanghai Jiaotong University, Shanghai 200240, China). p. 25—28

Abstract: A flexible manufacturing system of non-root chipping double-sided arc welding robots is studied in order to realize robot automatic welding for thick plate of low alloy high tensile steel. Master-slave coordinated method is adopted. Motoman robot is master and KUKA robot is slave. According to the ending position attitude of welding torch of master hand, reference path plane of plate is looked on as symmetric plane. Motion path of slave-hand is deduced by kinematics coordinate conversion. And Master-slave coordinated motion of double-sided arc welding robots is reached and is verified by coordinated motion experiment.

Key words: double-sided arc welding; double robots; master-slave control; coordinated motion

Comprehensive evaluation on effect of weld shape on mechanical performances by analytic hierarchy process

LIU Xin[2], LEI Yongping, GONG Shuili (1. Beijing University of Technology, Beijing 100010, China; 2. Science and Technology on Power Beam Processes Laboratory, Beijing Aeronautical Manufacturing Technology Research Institute, Beijing 100024, China). p. 29—32

Abstract: Four different weld shapes are obtained by proper electron beam welding parameters, which are respectively named as bell shape, funnel shape, nail shape and wedge shape. Mechanical performance of the electron beam welded joints with different shapes were carried. The influence of weld shape on mechanical performance of the joints was synthetically evaluated by analytic hierarchy mathematical model. The results show that weld shape effects tensile property, fatigue property and microhardness of the joint. The sequencing of mechanical performance of the joints with four different shapes by analytic hierarchy process is: bell shape, funnel shape, wedge shape, and nail shape. It is validated by experimental results that the analytic hierarchy mathematical model is effective and practical.

Key words: weld shape; electron beam welding; mechanical performance; analytic hierarchy process

Effects of welding parameters on weld geometry of pulsed Nd: YAG laser/TIG hybrid welding process of 304 stainless steel

ZHANG Linjie, ZHANG Jianxun, CAO Weijie, CHAI Guoming, GONG Shuili (1. State Key Laboratory of Mechanical Behavior for Materials, Xi'an Jiaotong University, Xi'an 710049, China; 2. National key Laboratory for High Energy Density Beam Processing Technology, Beijing Aeronautical Manufacturing Technology Research Institute, Beijing 100024, China). p. 33—36

Abstract: Effects of welding parameters on the weld geometry are investigated for pulsed Nd: YAG laser/TIG hybrid welding of 304 stainless steel plate. The results show that cross sectional area of hybrid weld is larger than the sum of cross sectional area of single laser weld and that of single TIG weld, which means synergetic effect occurs during hybrid welding process; weld width, weld depth, weld cross sectional area and heat transfer efficiency increase with the increase of laser power; when defocusing distance increase from -3mm to 5mm, weld width, weld depth, weld cross sectional area and heat transfer efficiency would increase and reach the maximum when defocus.